

## Columnar-to-Disk Structural Transition in Nanoscale $(\text{SiO}_2)_N$ Clusters

Stefan T. Bromley\*

*Departament de Química Física & Centre Especial de Recerca en Química Teòrica,  
Universitat de Barcelona & Parc Científic de Barcelona, C/ Martí i Franquès 1, E-08028 Barcelona, Spain*

Edwin Flikkema

*Ceramic Membrane Centre "The Pore," Delft University of Technology, Julianalaan 136, 2628 BL, Delft, The Netherlands*

(Received 7 March 2005; published 28 October 2005)

Extensive large-scale global optimizations refined by *ab initio* calculations are used to propose  $(\text{SiO}_2)_N$   $N = 14$ – $27$  ground states. For  $N < 23$  clusters are columnar and show  $N$ -odd– $N$ -even stability, energetically and electronically. At  $N = 23$  a columnar-to-disk structural transition occurs reminiscent of that observed for  $\text{Si}_N$ . These transitions differ in nature but have the same basis, linking the nanostructural behavior of an element (Si) and its oxide ( $\text{SiO}_2$ ). Considering the impact of devices based on the nanoscale manipulation of Si/ $\text{SiO}_2$  the result is of potential technological importance.

DOI: [10.1103/PhysRevLett.95.185505](https://doi.org/10.1103/PhysRevLett.95.185505)

PACS numbers: 61.46.+w, 36.40.Ei, 36.40.Mr, 68.65.–k

The technological importance of nanoscale silica ( $\text{SiO}_2$ ) can hardly be overstated considering its established utilization in microelectronics, catalysis, and composite materials and its promise in the emerging field of photonics. Although much experimental and theoretical work has focused upon the stabilities and structures of the many silica bulk polymorphs and their surfaces, the low energy structures and potential energy surface (PES) of nanoscale  $\text{SiO}_2$  clusters is relatively unknown. In this Letter we provide the beginnings of an energetic baseline of the complex PES of nanoscale  $\text{SiO}_2$  by finding the lowest energy forms of silica for  $(\text{SiO}_2)_N$   $N = 14$ – $27$  providing new limits on the stability of this centrally important material in the physical, chemical, and geophysical sciences. The clusters we study all have at least one dimension between 1 and 2.5 nm and are all substantially lower in energy than any previously reported. Our results strongly indicate that one-dimensional columnar structures are energetically favored up to a length scale of at least 2 nm where upon a transition to two-dimensional trigonal disk-like structures occurs at  $N = 23$ . The transition is characterized by sharp changes in measures of the structural form, electronic structure, and bonding topology of the cluster series, but appears smooth with respect to cluster energies. The structural transition in  $(\text{SiO}_2)_N$  clusters is compared to that known for clusters of its parent element  $\text{Si}_N$  [1]. In both cases for  $N = 23$ – $25$  a structural transition from elongated to more compact forms appears to occur in the thermodynamically preferred clusters [2]. Usually oxides and their parent elements display different but complementary physical and chemical properties and typically bear little structural relation to one another. Our finding that, at the nanoscale, the size-dependent structural behavior of  $\text{SiO}_2$  and its parent element follow a similar general pattern is at once relatively unexpected and fundamentally suggests an inherent link between the two materials. Because of the immense dependence on the combined

structural and physical properties of both nanoscale Si and  $\text{SiO}_2$  in electronic and optical devices, our demonstration of such a connection is of potential significant technological importance.

Although relatively small,  $M \leq 20$  homogeneous clusters of low atomic weight atoms are now within range of fully quantum mechanical global optimization studies [3], for the relatively large heterogeneous clusters studied herein [some with  $M > 80$ , where  $M = 3N$  for our  $(\text{SiO}_2)_N$  clusters] the PES is very complex and thus a less computationally demanding approach is essential, in part at least, to ensure some degree of tractability. For the case of model clusters with a single particle type interacting through a two-body Lennard-Jones potential, unbiased global optimization algorithms have managed to obtain ground state structures with a high degree of certainty for up to  $M \sim 200$  [4]. It is important to note that the complexity of our study with respect to such homogeneous cluster studies is further greatly complicated by two factors: (i) as our clusters possess two atom types, {Si, O}, and three two-body interactions, {Si-O, O-O, Si-Si}, the combinatorial complexity of the system is increased; (ii) as our potentials also incorporate long-range electrostatic interactions, all atoms interact significantly with all other atoms. Such factors, especially when considering a real material, make it particularly crucial that a well-parameterized potential set be employed to accurately represent the complex PES. For nanoscale silica we have found that commonly used bulk-parameterized potentials [5,6] are less accurate for small cluster systems [7]. The reason for this nanoscale breakdown is mainly due to the occurrence of defect states in nanoscale  $\text{SiO}_2$  not commonly found in bulk silica (e.g.,  $\text{Si}_2\text{O}_2$  two-rings,  $\text{Si}=\text{O}$  terminations). In order to more accurately represent the PES of small silica clusters we have thus developed our own specifically parameterized potential set [7] which retains the two-body Buckingham form complemented with electrostatics, as

successfully used in bulk parameterized  $\text{SiO}_2$  potentials [5,6]. Although our potential has been instrumental in successfully obtaining ground state candidates for  $(\text{SiO}_2)_N$   $N = 6-12$  [8] and for identifying the structures of magic  $(\text{SiO}_2)_8$ -based magic clusters observed in laser ablation experiments [9]—for the significantly larger  $(\text{SiO}_2)_N$   $N = 14-27$  clusters studied herein we also used the bulk-parameterized potential from Ref. [5]. Both potentials were combined with the basin-hopping (BH) global optimization algorithm [10] which uses a combination of Monte Carlo sampling and energy minimization to efficiently sample the immense space of cluster configurations by effectively removing barriers between neighboring minima. Although the BH algorithm is one of the least hindered global optimization methods with respect to the specific topology of the PES [11], to overcome problems of being trapped in local regions of phase space, it was found to be imperative that a selection of different starting structures be made to help ensure an even and extensive sampling [10]. For each BH run a number of randomly generated cluster structures, of the respective size, were used. We also found it essential to take selected low energy cluster structures from completed BH runs as starting points for subsequent runs, using relatively lower temperatures, to specifically sample low energy regions of phase space. Although potentials are very efficient and relatively accurate for generating many low energy  $\text{SiO}_2$  structures, they are inherently an approximate description of the electronically determined state of the system. The results of the BH runs were thus used as a good quality guide to the true isomer energy spectrum, which we then obtained by fully energy minimizing a low energy subset of candidate structures for each  $N$  using density functional theory (DFT). From each BH run we take a set containing at least the 20 lowest energy clusters and approximately 5–10 higher energy symmetric clusters for accurate DFT refinement. For DFT calculations the B3LYP hybrid exchange-correlation functional [12] with a 6–31G(d) basis set was used, employing no symmetry constraints. This level of theory has been shown in numerous previous studies to be suitable for calculating accurate structures and energies of  $\text{SiO}_2$  nanoclusters [13,14]. The GAMESS-UK [15] code was used for all DFT calculations.

The structures of the lowest energy clusters we obtain for  $(\text{SiO}_2)_N$   $N = 14-27$  are displayed in Fig. 1. An indication of the quality of the results from our method is given by examining the cluster energies [with respect to the composite atoms in their triplet state at a B3LYP/6-31G(d) level] with increasing size. The extrapolated limiting value [ $E(N) = E(\text{bulk}) + aN^{-b}$ ] of these energies gives a measure of the energetic stability of the clusters with respect to the thermodynamic limit of bulk  $\text{SiO}_2$ . In the large cluster regime many generic cluster properties show a regular dependence on  $N^{-1/3}$  (proportional to the fraction of surface atoms in an ideal spherical cluster)

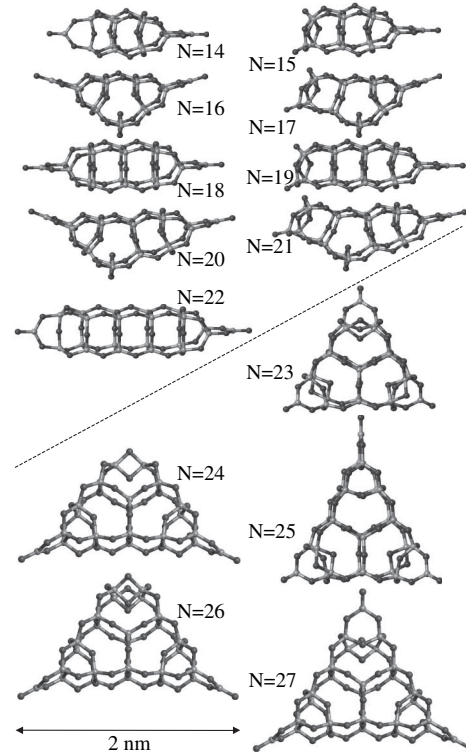


FIG. 1. Lowest energy  $(\text{SiO}_2)_N$  clusters,  $N = 14-27$  (dashed line separates the columnar and disklike clusters).

formally capturing the importance of high surface-to-volume ratios. For small  $\text{SiO}_2$  clusters ( $N < 13$ ) previous work indicates that this dependence is nonlinear and a fit with  $b > 1/3$  appears to better fit the data [16]. For the larger clusters studies herein (all with  $>40$  atoms) fitting the energies using  $b = 1/3$  results in a predicted limiting energy of 19.0 eV/ $\text{SiO}_2$  [see Fig. 2(a) where  $R^2 = 0.995$ ] in good correspondence with the experimentally measured energy of  $\alpha$ -quartz (19.2 eV/ $\text{SiO}_2$  [17]), giving confidence in the validity of our results. Using the fitted  $E(N)$  function, for approximately  $N > 7000$ , the energy with respect to  $\alpha$ -quartz becomes less than 0.3 eV/ $\text{SiO}_2$ . Within this energy range most currently known thermodynamically metastable bulk polymorphs of silica are known to exist giving a rough measure of the onset of bulk stability. Assuming a suitable silica density and taking clusters at this value of  $N$  to be spherical, we estimate that the  $\text{SiO}_2$  nanoscale-to-bulk transition occurs for a particle diameter of  $\sim 7$  nm.

One other study [18] has used a comparable methodology to ours to investigate  $(\text{SiO}_2)_N$  clusters for some clusters in the size range studied herein. Therein  $(\text{SiO}_2)_N$  clusters of the specific sizes  $N = 12, 22, 24, 45,$  and  $46$  were produced from molecular dynamics runs using a bulk-parameterized silica potential [6] and then energy minimized using DFT. Based upon this limited sampling with no strong bias towards low energy structures, it was proposed that clusters consist of end-on linked double

$\text{Si}_5\text{O}_5$  five-rings. We have calculated that this structural type is significantly higher ( $>1.75$  eV) in energy than our disklike structure for  $N = 24$ , ruling out this possibility. It is noted that our  $N = 24$  disklike ground state candidate cluster is also lower in energy ( $>1.5$  eV) than fully-coordinated  $(\text{SiO}_2)_{24}$   $N = 24$  cage constructions reported previously [16,19].

For the lowest energy clusters found in this work, the structural growth trend for  $(\text{SiO}_2)_N$   $N = 14$ –22 clusters is found to be remarkably simple and proceeds via the addition of  $\text{Si}_4\text{O}_4$  four-rings to make progressively longer columnar clusters (see Fig. 2). This nonbulklike pattern can be seen through  $N = 14, 18, 22$ , and  $N = 15, 19$ . For nanoclusters between these values of  $N$  the number of  $\text{SiO}_2$  units is not sufficient to make a column of complete four-rings and instead a  $\text{Si}_2\text{O}_2$  two-ring is inserted into the side of the cluster (e.g.,  $N = 16, 17, 20, 21$ ). For all columnar clusters the dominant defect termination is via  $\text{Si}=\text{O}$ , either at both ends of the column for even  $N$ , or only at one end for odd  $N$ . This termination appears to be energetically significantly favored over other terminations observed in higher energy isomers. For clusters  $N = 15, 17,$

19, 21, the odd number of  $\text{SiO}_2$  units does not allow for a two-fold symmetric termination with only  $\text{Si}=\text{O}$  groups, and the odd- $N$  columnar clusters are instead terminated by one  $\text{Si}=\text{O}$  defect and a less energetically favorable defect consisting of one singly coordinated and one triply coordinated oxygen center [8]. In all these cases, however, the connected four-ring columnar skeleton is maintained, which still appears to be the energetically favored structural route to obtain the lowest energy for this size range. The stability of nanoscale columnar  $(\text{SiO}_2)_N$  clusters possessing reactive defective ends naturally provides a route to linear coalescence, perhaps linked to the high temperature synthesis of silica nanowires [20].

The odd-even alternation in the  $(\text{SiO}_2)_N$  structure of the columns is also reflected in the progressive energetic change in adding a  $\text{SiO}_2$  unit to each cluster (the nucleation energy) given by  $E_{\text{nuc}} = E(N) - E(N-1) - E(\text{SiO}_2)$  [see Fig. 2(a)], and in the gap between the highest occupied molecular orbital (HOMO) and lowest unoccupied molecular orbitals (LUMO), which often indicates reactive stability [Fig. 2(b)]. The odd- $N$  dips in the alternating HOMO-LUMO trend are linked to the location of the frontier orbitals, which are localized around the energetically nonfavorable (i.e., non- $\text{Si}=\text{O}$ ) terminations for these columnar clusters.

Although persistent, the one-dimensional low energy columnar growth pattern is terminated at  $N = 23$  resulting in the emergence of a more compact two-dimensional disklike structure based on the centrally symmetric sharing of three double  $\text{Si}_5\text{O}_5$  five-ring cages. For the  $N$ -odd  $(\text{SiO}_2)_N$  clusters for  $N = 23$ , it appears that having one  $\text{Si}=\text{O}$  termination and one less energetically favored termination in a columnar cluster is outweighed by having three  $\text{Si}=\text{O}$  terminations and a more compact structure. For even  $N$  the energetic benefit of having a disklike form as opposed to a columnar form appears to be solely structural with both forms having the same double  $\text{Si}=\text{O}$  defect termination. The changes in internal cluster structure can be assessed by tracking the change in average ring size  $\langle R \rangle$  (where an  $R$ -ring denotes a ring containing  $R$  Si atoms); see Fig. 2(c). As the (strain) energy of a silica structure is known to depend upon  $\langle R \rangle$  [21], this measure allows for a topological analysis of the transition. For  $N = 14$ –22  $\langle R \rangle$  exhibits odd-even fluctuations much like the HOMO-LUMO gap and nucleation energy. For both odd and even sets of columnar clusters  $\langle R \rangle$  increases although it is seen to level off with increasing  $N$ . This suggests that columnar growth can only maintain a lowering of strain and subsequently an increasing binding energy consistent with the observed  $N^{-1/3}$  dependence over a small size range. At  $N = 23$  a significant increase in  $\langle R \rangle$  is observed corresponding to a columnar-to-disk transition showing how the disk form allows for less strained structures. For the nucleation energy [Fig. 2(a)] and HOMO-LUMO gap [Fig. 2(b)] a similar picture of the transition is also observed for  $N > 22$ . In each case the oscillatory pattern for

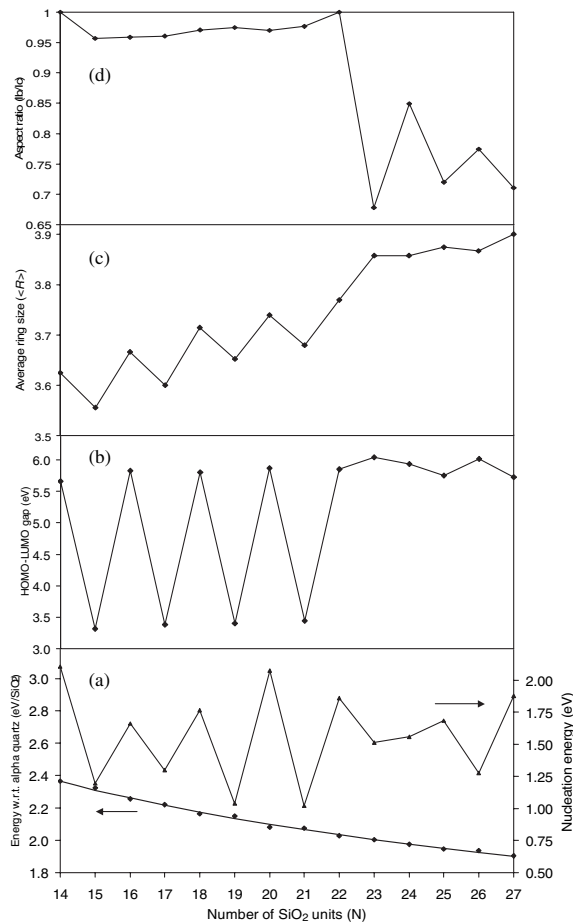


FIG. 2. For  $(\text{SiO}_2)_N$   $N = 14$ –27: (a) Cluster energies (eV/ $\text{SiO}_2$ ) with respect to the bulk extrapolated limit (left), nucleation energies (eV) (right). (b) HOMO-LUMO gap (eV). (c) Average  $(\text{SiO})_R$  ring size  $\langle R \rangle$ . (d) Aspect ratio ( $I_b/I_c$ ).

$N < 23$  stops giving rise to new behavior. For  $N = 23$ – $27$  the HOMO-LUMO gap remains constant and large consistent with the disk structures having more relaxed structures and only Si=O terminations. At the start of the disklike regime the nucleation energy also stabilizes and then, contrary to the columnar regime, is seen to be less favorable for the  $N$ -even  $N = 26$  disk. A further measure of the sharp transition between columns and disks is also shown in Fig. 2(d), where the eigenvalues ( $\lambda_1 \leq \lambda_2 \leq \lambda_3$ ) of the mass weighted gyration tensor of each cluster are used to provide a measure of the overall structural form of each cluster. The measure  $S$  given by  $(\lambda_1 + \lambda_3)/(\lambda_2 + \lambda_3)$ , which is equal to the ratio of inertial moments  $I_b/I_c$ ,  $I_a \leq I_b, \leq I_c$  quantifying the aspect ratio of each cluster ( $S = 1$ : perfect column,  $S = 0.5$ : perfect disk), shows how  $S$  abruptly decreases at  $N = 23$  from  $S \sim 1$  showing a transition to more disklike structures.

Although unlike the relatively simple growth behavior of closed packed clusters seen in many other systems (e.g., metals, rare gases), our predicted structural transition in  $(\text{SiO}_2)_N$  clusters is reminiscent of the prolate-to-spherical transition observed in small semiconducting  $\text{Si}_N$  clusters, occurring at  $N \sim 25$  [1]. The structural details of this transition were recently elucidated by a global optimization study [2] showing that the structures of midsized Si clusters are thermodynamically controlled. As well-defined  $\text{SiO}_2$  clusters may be produced via oxidizing silicon [22] we suggest that, via high temperature oxidation of  $\text{Si}_N$ , our predicted structural transition for low energy  $(\text{SiO}_2)_N$  clusters could be experimentally realized. Considering the differences in the structures of the predicted ground state silicon clusters [2] with those of the silicon skeletons of our respective predicted oxide clusters, it is unlikely that a simple structural isomorphism is responsible for their similar nanoscale behavior. Instead, a more likely reason is the directional bonding found in both systems. For the few elemental systems of this type (e.g., C [23], B [3], Si [1,2], Ge [24]) it has been established by experimental and theoretical means that structural transitions occur for nanoscale clusters. Most other elements form relatively densely packed clusters via isotropic interatomic interactions (e.g., metallic, dispersive) and do not display such rich structural behavior. Similarly isotropic ionic forces tend to dominate the interatomic bonding in the oxides of most elements and the clusters thus formed quickly reveal structures close to their respective bulk phases [25]. In a few rare cases both element and oxide may exhibit directional bonding at the nanoscale and thus both have the possibility to display such rich nanostructural behavior. For our case of Si and  $\text{SiO}_2$  the parallel structural behavior at the nanoscale is all the more pertinent as of all oxide/element pairs none has been pushed farther in terms of structural miniaturization and nanoscale integration through the drive for improved device technology. With imminent decreases in device size, knowledge of how both systems behave at the nanoscale will be imperative. It is our hope that our work will stimulate experiments into the

thermodynamically preferred forms of  $\text{SiO}_2$  clusters confirming our predictions.

We thank A. A. Sokol for useful discussions.

---

\*Corresponding author.

- [1] M. F. Jarrold and V. A. Constant, Phys. Rev. Lett. **67**, 2994 (1991).
- [2] K. A. Jackson, M. Horoi, I. Chaudhuri, T. Frauenheim, and A. A. Shvartsburg, Phys. Rev. Lett. **93**, 013401 (2004).
- [3] B. Kiran, S. Bulusu, H.-J. Zhai, S. Yoo, X. C. Zeng, and L.-S. Wang, Proc. Natl. Acad. Sci. U.S.A. **102**, 961 (2005).
- [4] J. Lee, I.-H. Lee, and J. Lee, Phys. Rev. Lett. **91**, 080201 (2003).
- [5] S. Tsuneyuki, M. Tsukada, H. Aoki, and Y. Matsui, Phys. Rev. Lett. **61**, 869 (1988).
- [6] B. W. H. Van Beest, G. K. Kramer, and R. A. van Santen, Phys. Rev. Lett. **64**, 1955 (1990).
- [7] E. Flikkema and S. T. Bromley, Chem. Phys. Lett. **378**, 622 (2003).
- [8] E. Flikkema and S. T. Bromley, J. Phys. Chem. B **108**, 9638 (2004).
- [9] S. T. Bromley and E. Flikkema, J. Chem. Phys. **122**, 114303 (2005).
- [10] D. J. Wales and J. P. K. Doye, J. Phys. Chem. **101**, 5111 (1997).
- [11] J. P. K. Doye and D. J. Wales, Phys. Rev. Lett. **80**, 1357 (1998).
- [12] A. D. J. Becke, J. Phys. Chem. **98**, 5648 (1993).
- [13] W. C. Lu, C. Z. Wang, V. Hguyen, M. W. Schmidt, M. S. Gordon, K. M. Ho, J. Phys. Chem. A, **107**, 6936 (2003).
- [14] T. S. Chu, R. Q. Zhang, and H. F. Cheung, J. Phys. Chem. B **105**, 1705 (2001).
- [15] Computer code GAMESS-UK is a package of *ab initio* programs written by M. F. Guest, J. H. van Lenthe, J. Kendrick, and P. Sherwood, with contributions from R. D. Amos, R. J. Buenker, H. van Dam, M. Dupuis, N. C. Handy, I. H. Hillier, P. J. Knowles, V. Bonacic-Koutecky, W. von Niessen, R. J. Harrison, A. P. Rendell, V. R. Saunders, K. Schoffel, A. J. Stone, and D. Tozer.
- [16] S. T. Bromley, Nano Lett. **4**, 1427 (2004).
- [17] *CRC Handbook of Chemistry and Physics*, edited by D. R. Lide (CRC Press, Boca Raton, 2004), 85th ed..
- [18] J. Song and M. Choi, Phys. Rev. B **65**, 241302 (2002).
- [19] D. Zhang, M. Zhao, and R. Q. Zhang, J. Phys. Chem. B **108**, 18451 (2004).
- [20] D. P. Yu, Q. L. Hang, Y. Ding, H. Z. Zhang, Z. G. Bai, J. J. Wang, Y. H. Zou, W. Qian, G. C. Xiong, and S. Q. Feng, Appl. Phys. Lett. **73**, 3076 (1998).
- [21] M. A. Zwijnenburg, S. T. Bromley, J. C. Jansen, and Th. Maschmeyer, Chem. Mater. **16**, 12 (2004).
- [22] L. S. Wang, J. B. Nicholas, M. Dupuis, H. B. Wu, and S. D. Colson, Phys. Rev. Lett. **78**, 4450 (1997).
- [23] A. V. Orden and R. J. Saykally, Chem. Rev. **98**, 2313 (1998).
- [24] J. M. Hunter, J. L. Fye, M. F. Jarrold, and J. E. Bower, Phys. Rev. Lett. **73**, 2063 (1994).
- [25] F. Calvo, Phys. Rev. B **67**, 161403(R) (2003).